

Two-loop massless QCD corrections to the $g + g \rightarrow H + H$ four-point amplitude

Pulak Banerjee,^a Sophia Borowka,^b Prasanna K. Dhani,^a Thomas Gehrmann,^c and V. Ravindran^a

^a*The Institute of Mathematical Sciences, HBNI, Taramani, Chennai-600113, India*

^b*Theoretical Physics Department, CERN, CH-1211 Geneva, Switzerland*

^c*Physik-Institut, Universität Zürich, Winterthurerstrasse 190, CH-8057 Zürich, Switzerland*

E-mail: bpulak@imsc.res.in, sophia.borowka@cern.ch,
prasannakd@imsc.res.in, thomas.gehrmann@uzh.ch, ravindra@imsc.res.in

ABSTRACT: We compute the two-loop massless QCD corrections to the four-point amplitude $g + g \rightarrow H + H$ resulting from effective operator insertions that describe the interaction of a Higgs boson with gluons in the infinite top quark mass limit. This amplitude is an essential ingredient to the third-order QCD corrections to Higgs boson pair production. We have implemented our results in a numerical code that can be used for further phenomenological studies.

KEYWORDS: QCD, Higgs boson, Loop amplitudes, LHC

Contents

1	Introduction	1
2	Virtual Higgs Pair Production Contributions to N³LO	2
2.1	Higgs effective field theory	2
2.2	Kinematics	3
2.3	Tensors and projectors	4
2.4	Diagrams to $\mathcal{O}(a_s^4)$	4
2.5	Ultraviolet renormalization and operator mixing	7
2.6	Infrared factorization	8
3	Calculation of the Amplitude	9
4	Numerical Evaluation of the Two-loop Amplitudes	10
5	Discussion and Conclusions	11

1 Introduction

The discovery of the Higgs boson at the Large Hadron Collider [1, 2] is an important milestone in particle physics. It puts the Standard Model (SM) in a firm position to describe the dynamics of all the known elementary particles. Of course, there are several shortcomings in the SM which lead physicists to explore physics beyond the SM. There have been tremendous efforts to construct models that address these shortcomings and at the same time demonstrate rich phenomenology that can be explored at present and future colliders. All these culminated into dedicated experimental searches for hints of new physics which in turn constrain the parameters of beyond the SM scenarios [3].

By measuring the mass of the Higgs boson, one can predict the trilinear self-coupling in the Higgs sector of the SM. This is a crucial parameter that describes the shape of the Higgs potential. In order to better understand the Higgs sector and the nature of the electroweak symmetry breaking mechanism, it is important to measure this self-coupling independently. At hadron colliders, one of the potential channels that can probe this self-coupling is the production of a pair of Higgs bosons [4–7]. The dominant production channel in the SM is through the loop-induced gluon fusion subprocess [8, 9]. At leading order (LO), this process involves two mechanisms, with the scattering amplitude for one of the them depending on the trilinear Higgs boson coupling. Since both mechanisms are loop-induced through heavy quarks and there is destructive interference between their respective amplitudes, the SM production cross section at LHC energies is only few tens of a femtobarn. In addition, a large and irreducible background [10–15] makes its detection an experimentally demanding

task. Double Higgs boson production can receive substantial contributions from physics processes beyond the SM, and there are already several detailed studies indicating scenarios for a substantial increase in its production rate (see [16] and the references therein).

Theoretically, it is a challenging task to compute higher order QCD effects when taking into account the exact top quark mass dependence, since the Born-level contribution appears only at one loop. The first computation of next-to-leading order (NLO) QCD corrections was performed in the infinite top quark mass limit in [4]. In this limit, the top quark is integrated out, resulting in a field theory that contains effective operators coupling the Higgs field to the gluon field. These early results were then improved upon by considering various NLO contributions from finite top quark mass effects [17–22]. Recently, the full NLO corrections with exact top quark mass dependence could be completed [23, 24], owing to technical progress in the numerical evaluation of two-loop integrals and amplitudes with internal masses. At next-to-next-to-leading order (NNLO) level, results are available only in the heavy top limit. The prediction at NNLO level in the soft plus virtual (SV) approximation can be found in [25], the leading top quark mass corrections were then included in [26], while in [27] the impact of the remaining hard contributions were studied. The relevant Wilson coefficients at NNLO were obtained in [28]. For the fully differential results at NNLO level, see [29–31]. By using a re-weighting approach, these fixed-order NNLO results for infinite top quark mass can be combined with the exact NLO top quark mass dependence to quantify [32] the top quark mass effects at NNLO. Effects of threshold resummation at next-to-next-to-leading logarithm (NNLL) level using soft collinear effective theory were obtained in [31, 33].

Going beyond NNLO level in QCD is a challenging task owing to the technical difficulties involved in computing the loop integrals for the virtual subprocesses and the phase space integrals when there are real emissions. In this article we make a first step towards computing the third-order correction to the production of a pair of Higgs bosons in the gluon initiated channels. In particular we compute virtual amplitudes for the subprocess $g + g \rightarrow H + H$, resulting from two effective operator insertions, at the two-loop level. The paper is structured as follows. In Section 2, we introduce the notation, describe the effective field theory that results in the limit of an infinite top quark mass, and discuss the different purely virtual contributions to Higgs boson pair production up to next-to-next-to-next-to-leading order (N³LO). Section 3 describes in detail the calculation of the two-loop amplitude for $g + g \rightarrow H + H$, and the numerical evaluation of the results is discussed in 4. We conclude with an outlook on future applications in Section 5.

2 Virtual Higgs Pair Production Contributions to N³LO

2.1 Higgs effective field theory

We compute the relevant amplitudes in an effective theory where the top quark degrees of freedom are integrated out. The effective Lagrangian that describes the coupling of one and two Higgs bosons to gluons is given by

$$\mathcal{L}_{eff} = -\frac{1}{4} \left(C_H(a_s) \frac{\phi}{v} - C_{HH}(a_s) \frac{\phi^2}{v^2} \right) G_{\mu\nu} G^{\mu\nu}, \quad (2.1)$$

where $G_{\mu\nu}$ denotes the gluon field strength tensor, ϕ , the Higgs boson and $v = 246$ GeV is the vacuum expectation value of the Higgs field. Note that we have taken only those terms in the \mathcal{L}_{eff} into account that are relevant for the production of two Higgs bosons in a gluon-gluon initiated process. The constants C_H and C_{HH} are the Wilson coefficients [28, 34–38] determined by matching the effective theory to the full theory and they can be expanded in powers of the renormalized strong coupling constant $a_s = g_s^2(\mu_R^2)/(16\pi^2) = \alpha_s(\mu_R^2)/(4\pi)$ with μ_R the renormalisation scale,

$$\begin{aligned}
C_H(a_s) = & -\frac{4a_s}{3} \left[1 + a_s(11) \right. \\
& + a_s^2 \left(\left\{ \frac{2777}{18} + 19 \log \left(\frac{\mu_R^2}{m_t^2} \right) \right\} + n_f \left\{ -\frac{67}{6} + \frac{16}{3} \log \left(\frac{\mu_R^2}{m_t^2} \right) \right\} \right) \\
& + a_s^3 \left(-\frac{2892659}{648} + \frac{3466}{9} \log \left(\frac{\mu_R^2}{m_t^2} \right) + 209 \log^2 \left(\frac{\mu_R^2}{m_t^2} \right) + \frac{897943}{144} \zeta_3 \right. \\
& + n_f \left\{ \frac{40291}{324} + \frac{1760}{27} \log \left(\frac{\mu_R^2}{m_t^2} \right) + 46 \log^2 \left(\frac{\mu_R^2}{m_t^2} \right) - \frac{110779}{216} \zeta_3 \right\} \\
& \left. \left. + n_f^2 \left\{ -\frac{6865}{486} + \frac{77}{27} \log \left(\frac{\mu_R^2}{m_t^2} \right) - \frac{32}{9} \log^2 \left(\frac{\mu_R^2}{m_t^2} \right) \right\} \right) \right], \quad (2.2)
\end{aligned}$$

$$\begin{aligned}
C_{HH}(a_s) = & -\frac{4a_s}{3} \left[1 + a_s(11) \right. \\
& \left. + a_s^2 \left(\frac{3197}{18} + 19 \log \left(\frac{\mu_R^2}{m_t^2} \right) + n_f \left\{ -\frac{1}{2} + \frac{16}{3} \log \left(\frac{\mu_R^2}{m_t^2} \right) \right\} \right) \right], \quad (2.3)
\end{aligned}$$

and where n_f is the number of light flavors, m_t is the \overline{MS} top quark mass at scale μ_R and $N = 3$ is fixed for QCD.

2.2 Kinematics

Consider the production of a pair of Higgs bosons in the gluon fusion subprocess,

$$g(p_1) + g(p_2) \rightarrow H(p_3) + H(p_4), \quad (2.4)$$

where p_1 and p_2 are the momenta of the incoming gluons, and p_3 and p_4 the momenta for the outgoing Higgs bosons, respectively. The Mandelstam variables for the above process are given by

$$s = (p_1 + p_2)^2, \quad t = (p_1 - p_3)^2, \quad u = (p_2 - p_3)^2. \quad (2.5)$$

They satisfy $s + t + u = 2m_h^2$ where m_h is the mass of the Higgs boson. In the following, we describe the computation of the one- and two-loop QCD corrections to the amplitude given in Eq. (2.4). We find that it is convenient to express this amplitude in terms of the dimensionless variables x , y and z

$$s = m_h^2 \frac{(1+x)^2}{x}, \quad t = -m_h^2 y, \quad u = -m_h^2 z. \quad (2.6)$$

2.3 Tensors and projectors

Using gauge invariance, the amplitude can be decomposed in terms of two second rank Lorentz tensors $\mathcal{T}_i^{\mu\nu}$ with $i = 1, 2$ as follows [8]:

$$\mathcal{M}_{ab}^{\mu\nu} = \delta_{ab} (\mathcal{T}_1^{\mu\nu} \mathcal{M}_1 + \mathcal{T}_2^{\mu\nu} \mathcal{M}_2) , \quad (2.7)$$

where the tensors are given by

$$\mathcal{T}_1^{\mu\nu} = g^{\mu\nu} - \frac{1}{p_1 \cdot p_2} (p_1^\nu p_2^\mu) \quad (2.8)$$

$$\mathcal{T}_2^{\mu\nu} = g^{\mu\nu} + \frac{1}{p_1 \cdot p_2 p_T^2} (m_h^2 p_2^\mu p_1^\nu - 2p_1 \cdot p_3 p_2^\mu p_3^\nu - 2p_2 \cdot p_3 p_3^\mu p_1^\nu + 2p_1 \cdot p_2 p_3^\mu p_3^\nu) , \quad (2.9)$$

with $p_T^2 = (tu - m_h^4)/s$. In color space, the amplitude is diagonal in the indices (a, b) of the incoming gluons. The scalar functions \mathcal{M}_i can be obtained from $\mathcal{M}_{ab}^{\mu\nu}$ by using appropriate projectors as follows

$$\mathcal{M}_i = \frac{1}{N^2 - 1} P_i^{\mu\nu} \mathcal{M}_{\mu\nu}^{ab} \delta_{ab}, \quad i = 1, 2, \quad (2.10)$$

where the projectors in d dimensions are given by,

$$\begin{aligned} P_1^{\mu\nu} &= \frac{1}{4} \frac{d-2}{d-3} \mathcal{T}_1^{\mu\nu} - \frac{1}{4} \frac{d-4}{d-3} \mathcal{T}_2^{\mu\nu} , \\ P_2^{\mu\nu} &= -\frac{1}{4} \frac{d-4}{d-3} \mathcal{T}_1^{\mu\nu} + \frac{1}{4} \frac{d-2}{d-3} \mathcal{T}_2^{\mu\nu} . \end{aligned} \quad (2.11)$$

2.4 Diagrams to $\mathcal{O}(a_s^4)$

When considering higher order massless QCD corrections to the $g+g \rightarrow H+H$ amplitudes in the effective theory, we encounter two topologically distinct classes of subprocesses we call Class-A and Class-B hereafter. We perform an expansion in a_s to include all the contributing diagrams.

- Class-A, see Fig. 1, contains diagrams where two Higgs bosons couple to each other and to gluons. They either couple to the gluons directly through a C_{HH} Wilson coefficient (left-hand column of Fig. 1), or through a Higgs boson propagator and the C_H Wilson coefficient (right-hand column of Fig. 1). The latter diagrams are linearly proportional to the triple Higgs coupling λ .
- Class-B, see Fig. 2, contains diagrams where Higgs bosons couple to two gluons through the effective vertices proportional to C_H , but do not couple to each other.

Both Wilson coefficients C_H and C_{HH} start at order a_s . Consequently, to LO in a_s only Class-A diagrams contribute. Beyond LO, that is from order a_s^2 onwards, the class-A diagrams are only of form factor type and the results for class-A to a_s^4 can be readily obtained from the three loop form factor [39, 40] that appears in purely virtual contributions to single Higgs boson production. The class-B diagrams start contributing from order a_s^2 ,

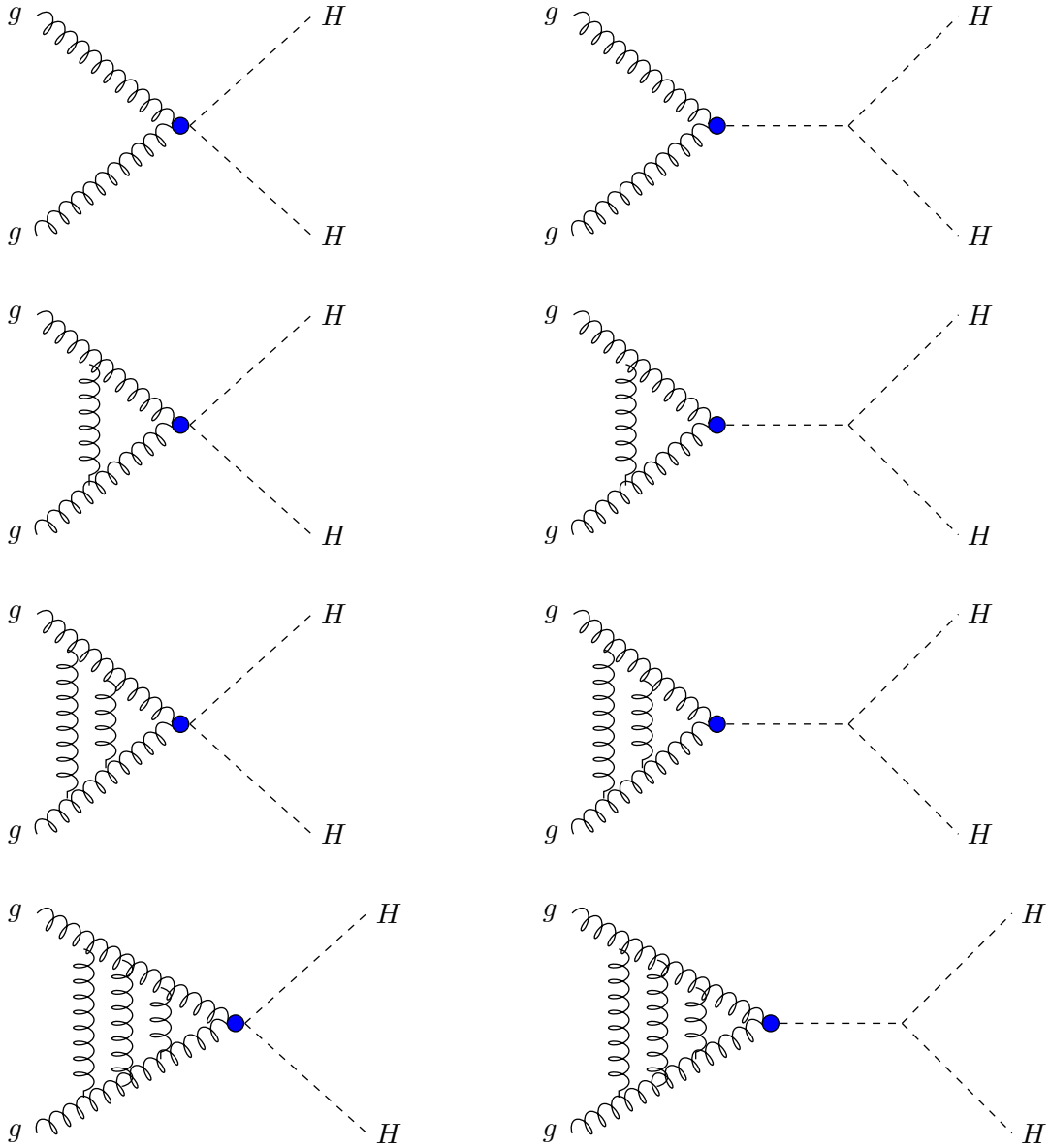


Figure 1: Class-A: Tree, one-, two- and three-loop amplitudes

with results only available up to order a_s^3 [4]. In the following, we will complete the a_s^4 contributions to the $g + g \rightarrow H + H$ amplitude, by computing the class-B diagrams to this order, which amount to their two-loop corrections.

In general, the scalar amplitudes \mathcal{M}_i can be written as a sum of amplitudes resulting from the two classes A and B

$$\mathcal{M}_i = \mathcal{M}_i^A + \mathcal{M}_i^B, \quad i = 1, 2. \quad (2.12)$$

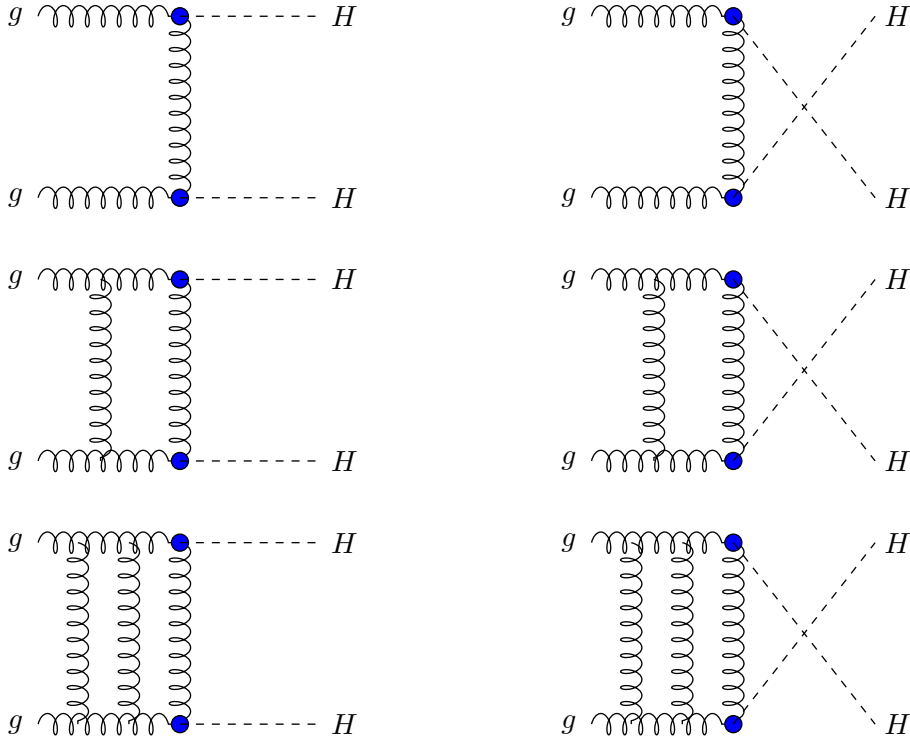


Figure 2: Class-B: Tree, one- and two-loop amplitudes

Since the \mathcal{M}_i^A are proportional to the Higgs boson form factor, they can be expressed as

$$\mathcal{M}_i^A = \delta_{i1} \overline{\mathcal{M}}_1^A(a_s) \sum_{j=0}^{\infty} a_s^j \mathcal{F}^{(j)}(d), \quad (2.13)$$

where

$$\overline{\mathcal{M}}_1^A(a_s) = i \frac{s}{2} \left(C_{HH}(a_s) - C_H(a_s) \frac{6\lambda v^2}{s - m_h^2} \right). \quad (2.14)$$

The amplitude \mathcal{M}_2^A is identically to zero to all orders in perturbation theory due to the choice of the tensorial basis. The form factors $\mathcal{F}^{(j)}(d)$ for $j = 1, 2, 3$ are known in the literature [39, 40].

In this article, the amplitudes of class-B are presented up to two loop level in perturbative QCD. At each order, the amplitude contains a pair of vertices resulting from the first term of the effective Lagrangian \mathcal{L}_{eff} and hence will be proportional to the square of the Wilson coefficient $C_H(a_s)$, expanded to the desired accuracy in a_s . Beyond leading order, the one- and two-loop diagrams are not only ultraviolet (UV) divergent but also infrared (IR) divergent resulting from soft and collinear regions of the loop momenta. We use dimensional regularization to treat both UV and IR divergences and all the divergences show up as poles in ϵ , where the space time dimension is $d = 4 - 2\epsilon$.

2.5 Ultraviolet renormalization and operator mixing

The bare strong coupling constant in the regularized theory is denoted by \hat{a}_s which is related to its renormalized counter-part by

$$\begin{aligned}\hat{a}_s \mu^{2\epsilon} S_\epsilon &= a_s \mu_R^{2\epsilon} Z(\mu_R^2) \\ &= a_s \mu_R^{2\epsilon} \left[1 - a_s \left(\frac{\beta_0}{\epsilon} \right) + a_s^2 \left(\frac{\beta_0^2}{\epsilon^2} - \frac{\beta_1}{2\epsilon} \right) + \mathcal{O}(a_s^3) \right],\end{aligned}\quad (2.15)$$

where $S_\epsilon = \exp[(\ln 4\pi - \gamma)\epsilon]$ with $\gamma \approx 0.5772\dots$ the Euler-Mascheroni constant. The beta function coefficients β_0 and β_1 are given by

$$\begin{aligned}\beta_0 &= \frac{11}{3}C_A - \frac{4}{3}T_F n_f, \\ \beta_1 &= \frac{34}{3}C_A^2 - 4T_F n_f C_F - \frac{20}{3}T_F n_f C_A,\end{aligned}\quad (2.16)$$

for the SU(N) color factors we have

$$C_A = N, \quad C_F = \frac{N^2 - 1}{2N}, \quad \text{and} \quad T_F = \frac{1}{2}.\quad (2.17)$$

Besides coupling constant renormalisation, the amplitudes also require the renormalisation of the effective operators in the effective Lagrangian, Eq. (2.1). Both composite operators that appear in our one- and two-loop amplitudes can develop UV divergences and thus have to undergo renormalisation, as derived in detail in [41]. In particular, a new renormalisation constant Z_{11}^L is needed in a counter term proportional to $G_{\mu\nu}G^{\mu\nu}\phi\phi$ to renormalize the additional UV divergence resulting from amplitudes involving two $G_{\mu\nu}G^{\mu\nu}\phi$ type operators starting from 2-loop order in class-B amplitudes. If we denote the amplitudes computed in the bare theory by $\hat{\mathcal{M}}_i^B$, then the relation between these bare amplitudes and the UV renormalized ones is given by

$$\mathcal{M}_i^B = Z_{\mathcal{O}}^2 \hat{\mathcal{M}}_i^B + Z_{11}^L \hat{\mathcal{M}}_i^{A,(0)} \Big|_{\lambda=0},\quad (2.18)$$

where $\hat{\mathcal{M}}_i^{A,(0)}$ is the Born amplitude from class-A and $\hat{\mathcal{M}}_i^B$ are the unrenormalized amplitudes from class-B. The latter can be expanded in powers of the unrenormalized coupling constant \hat{a}_s as

$$\hat{\mathcal{M}}_i^B = \hat{\mathcal{M}}_i^{B,(0)} + \left(\hat{a}_s \mu^{2\epsilon} S_\epsilon\right) \hat{\mathcal{M}}_i^{B,(1)} + \left(\hat{a}_s \mu^{2\epsilon} S_\epsilon\right)^2 \hat{\mathcal{M}}_i^{B,(2)} + \mathcal{O}(\hat{a}_s^3).\quad (2.19)$$

The overall renormalisation constant [42–44] is given by

$$Z_{\mathcal{O}} = 1 - a_s \left(\frac{1}{\epsilon} r_{\mathcal{O}_{1;1}} \right) + a_s^2 \left(\frac{1}{\epsilon^2} r_{\mathcal{O}_{2;2}} - \frac{1}{\epsilon} r_{\mathcal{O}_{2;1}} \right) + \mathcal{O}(a_s^3),\quad (2.20)$$

where

$$r_{\mathcal{O}_{1;1}} = \beta_0, \quad r_{\mathcal{O}_{2;2}} = \beta_0^2, \quad r_{\mathcal{O}_{2;1}} = \beta_1,$$

and Z_{11}^L is given by [41],

$$Z_{11}^L = a_s^2 \frac{\beta_1}{\epsilon} + \mathcal{O}(a_s^3). \quad (2.21)$$

The UV renormalized amplitude \mathcal{M}_i^B can be expanded in powers of a_s up to the two-loop level as follows:

$$\mathcal{M}_i^B = \mathcal{M}_i^{B,(0)} + a_s \mathcal{M}_i^{B,(1)} + a_s^2 \mathcal{M}_i^{B,(2)} + \mathcal{O}(a_s^3), \quad (2.22)$$

where,

$$\begin{aligned} \mathcal{M}_i^{B,(0)} &= \hat{\mathcal{M}}_i^{B,(0)}, \\ \mathcal{M}_i^{B,(1)} &= \mu_R^{2\epsilon} \left[\hat{\mathcal{M}}_i^{B,(1)} - \frac{1}{\mu_R^{2\epsilon}} \left(\frac{1}{\epsilon} 2r_{\mathcal{O}_{1;1}} \right) \hat{\mathcal{M}}_i^{B,(0)} \right], \\ \mathcal{M}_i^{B,(2)} &= \mu_R^{4\epsilon} \left[\hat{\mathcal{M}}_i^{B,(2)} - \frac{1}{\mu_R^{2\epsilon}} \left(\frac{1}{\epsilon} (2r_{\mathcal{O}_{1;1}} + \beta_0) \right) \hat{\mathcal{M}}_i^{B,(1)} \right. \\ &\quad + \frac{1}{\mu_R^{4\epsilon}} \left(\frac{1}{\epsilon^2} (r_{\mathcal{O}_{1;1}}^2 + 2r_{\mathcal{O}_{2;2}}) - \frac{1}{\epsilon} (2r_{\mathcal{O}_{2;1}}) \right) \hat{\mathcal{M}}_i^{B,(0)} \\ &\quad \left. + \frac{1}{\mu_R^{4\epsilon}} \left(\frac{\beta_1}{\epsilon} \right) \hat{\mathcal{M}}_i^{A,(0)} \Big|_{\lambda=0} \right]. \end{aligned} \quad (2.23)$$

In summary, the UV divergences that appear at the one- and two-loop level can be removed using coupling constant renormalisation through Z and the overall operator and the contact renormalisation constants, $Z_{\mathcal{O}}$ and Z_{11}^L respectively.

2.6 Infrared factorization

The resulting UV finite amplitudes will contain divergences of infrared origin, which remain as poles in the dimensional regularization parameter ϵ . These will cancel when combined with the real emission processes to compute observables. While these divergences disappear in the physical observables, the amplitudes beyond leading order demonstrate a very rich universal structure in the IR region. Catani [45] predicted IR divergences for n -point two-loop amplitudes in terms of certain universal IR anomalous dimensions, exploiting the iterative structure of the IR singular parts in any UV renormalized amplitudes in QCD. These could be related [46] to the factorization and resummation properties of QCD amplitudes, and were subsequently generalized to higher loop order [47, 48]. Following [45], we obtain

$$\begin{aligned} \mathcal{M}_i^{B,(0)} &= \mathcal{M}_i^{B,(0)} \\ \mathcal{M}_i^{B,(1)} &= 2\mathbf{I}_g^{(1)}(\epsilon) \mathcal{M}_i^{B,(0)} + \mathcal{M}_i^{B,(1),fin} \\ \mathcal{M}_i^{B,(2)} &= 4\mathbf{I}_g^{(2)}(\epsilon) \mathcal{M}_i^{B,(0)} + 2\mathbf{I}_g^{(1)}(\epsilon) \mathcal{M}_i^{B,(1)} + \mathcal{M}_i^{B,(2),fin} \end{aligned} \quad (2.24)$$

where $\mathbf{I}_g^{(1)}(\epsilon)$, $\mathbf{I}_g^{(2)}(\epsilon)$ are the IR singularity operators given by

$$\mathbf{I}_g^{(1)}(\epsilon) = -\frac{e^{\epsilon\gamma}}{\Gamma(1-\epsilon)} \left(\frac{C_A}{\epsilon^2} + \frac{\beta_0}{2\epsilon} \right) \left(-\frac{\mu_R^2}{s} \right)^\epsilon,$$

$$\mathbf{I}_g^{(2)}(\epsilon) = -\frac{1}{2}\mathbf{I}_g^{(1)}(\epsilon) \left[\mathbf{I}_g^{(1)}(\epsilon) + \frac{\beta_0}{\epsilon} \right] + \frac{e^{-\epsilon\gamma}\Gamma(1-2\epsilon)}{\Gamma(1-\epsilon)} \left[\frac{\beta_0}{2\epsilon} + K \right] \mathbf{I}_g^{(1)}(2\epsilon) + 2\mathbf{H}_g^{(2)}(\epsilon), \quad (2.25)$$

with

$$K = \left(\frac{67}{18} - \zeta_2 \right) C_A - \frac{10}{9} T_F n_f,$$

$$\mathbf{H}_g^{(2)}(\epsilon) = - \left(-\frac{\mu_R^2}{s} \right)^{2\epsilon} \frac{e^{\epsilon\gamma}}{\Gamma(1-\epsilon)} \times \frac{1}{2\epsilon} \left\{ C_A^2 \left(-\frac{5}{24} - \frac{11}{48}\zeta_2 - \frac{1}{4}\zeta_3 \right) + C_A n_f \left(\frac{29}{54} + \frac{1}{24}\zeta_2 \right) - \frac{1}{4} C_F n_f - \frac{5}{54} n_f^2 \right\}. \quad (2.26)$$

It is known that the terms that become finite or vanish as ϵ goes to zero, i.e., $\mathcal{O}(\epsilon^\alpha)$, $\alpha \geq 0$ in the subtraction operators $\mathbf{I}_g^{(1)}$ and $\mathbf{I}_g^{(2)}$ are arbitrary and they define the scheme in which these IR divergences are subtracted to obtain IR finite parts of amplitudes, $\mathcal{M}_i^{B,(j),fin}$. These scheme-dependent terms in the finite part of virtual contributions will cancel against those coming from the soft gluon emission subprocesses at the observable level. The only scheme dependence that will be left in a physical subprocess coefficient function is then due to the subtraction of collinear initial state divergences through mass factorization, parametrized by a factorization scale μ_F .

3 Calculation of the Amplitude

For the amplitudes of class-B, we needed to consider only those diagrams which involve a pair of vertices resulting from the first term of the effective Lagrangian and hence all the amplitudes are proportional to C_H^2 . These Feynman diagrams up to two-loop level were obtained with help of the package QGRAF [49]. There are 2 diagrams at tree level, 37 at one loop and 865 at two-loop order in perturbation theory. The output from QGRAF was then used for further algebraic manipulations involving traces of Dirac matrices, contraction of Lorentz and color indices, using two independent sets of in-house routines based on a symbolic package FORM [50]. The entire manipulations were performed in $d = 4 - 2\epsilon$ dimensions and most of the algebraic simplifications were done at this stage. We used the Feynman gauge throughout and hence allowed ghost particles in the loops. External ghosts are not required due to the transversal nature of the tensorial projectors Eq. (2.11).

At this stage, we obtain a large number of Feynman integrals with different sets of propagators and each containing scalar products of the independent external and internal momenta. Using the REDUZE2 package [51], we can identify the momentum shifts that are required to express each diagram in terms of a standard set of propagators (called auxiliary topology). The auxiliary topologies in the two-loop corrections to the class-B process are identical to those in equal-mass on-shell vector boson pair production at this loop order. They are described in [52] and were used to compute the two-loop corrections to $q\bar{q} \rightarrow VV$ in [53, 54]. They were subsequently extended towards non-equal gauge boson masses [55–58].

It is well known that the resulting Feynman integrals are not all independent and hence they can be expressed in terms of fewer scalar integrals, called Master Integrals (MIs) by using integration-by-parts (IBP) identities [59, 60]. Further simplifications can be done by exploiting the Lorentz invariance of the integrands, resulting in Lorentz invariance (LI) identities [61]. These identities can be solved systematically using lexicographic ordering (Laporta algorithm, [62]) to express any Feynman integral in terms of master integrals. These are implemented in several specialized computer algebra packages, for example AIR [63], FIRE [64], REDUZE2 [51, 65] and LiteRed [66], to perform suitable integral reductions such that one ends up with only MIs. We performed two independent reductions of the integrals in the two-loop class-B amplitude, one based on the Mathematica based package LiteRed [66] and the other based on REDUZE2 [51]. Counting kinematical crossings as independent integrals, we can express the one-loop amplitude in terms of 10 master integrals, while the two-loop amplitude contains 149 master integrals. These master integrals are two-loop four-point functions with internal massless propagators and two massive external legs of equal mass. They were computed analytically as Laurent series expansion in ϵ in [52, 67].

These MIs were then expressed in terms of generalized harmonic polylogarithms. An alternative functional basis can be obtained in terms of logarithms, polylogarithms $\text{Li}_{n \leq 4}$ and the multiple polylogarithm $\text{Li}_{2,2}$ by matching the original expression at the symbol level [52]. We use the master integrals in this latter representation. Substituting the MIs from [52, 67], we obtain the bare amplitudes $\hat{\mathcal{M}}_i^{B,(1)}$ and $\hat{\mathcal{M}}_i^{B,(2)}$. The ultraviolet singularities present in these amplitudes are removed by renormalisation as described in Section 2.5 above. The resulting UV renormalized amplitudes contain only infrared divergences. We find that the poles of these amplitudes agree with what is expected from IR factorization, Eq. (2.24), using the subtraction operators of Eq. (2.25). These define the finite remainders of the amplitudes $\mathcal{M}_i^{B,(j),fin}$ with $j = 0, 1, 2$.

4 Numerical Evaluation of the Two-loop Amplitudes

The finite remainders $\mathcal{M}_i^{B,(j),fin}$, $i = 1, 2$, computed in the previous section, are expressed in terms of multiple classical polylogarithms with arguments depending on the scaling variables x, y and their coefficients further depending on the Higgs mass m_h . Since the analytical results are too long to be presented in this article, we have provided ancillary files containing the analytical results (and their numerical evaluation) in Mathematica format. In order to demonstrate the dependence of the two-loop finite remainders on the scaling variables x and y for $m_h = 125$ GeV and with $\mu_R^2 = m_h^2/2$, we plot real and imaginary parts of both $\mathcal{M}_i^{B,(2),fin}$, $i = 1, 2$ as a function of the partonic invariant mass variable x for different choices of $\cos(\theta)$, where θ is the angle between one of the Higgs bosons in the final state and one of the initial gluons in their center of mass frame. We extract an additional factor of m_h^2 in the plots. The amplitude is invariant under $\cos(\theta) \rightarrow -\cos(\theta)$, as expected for a purely bosonic amplitude. Since this symmetry has not been used in the setup of the calculation, it serves as a strong check on our results.

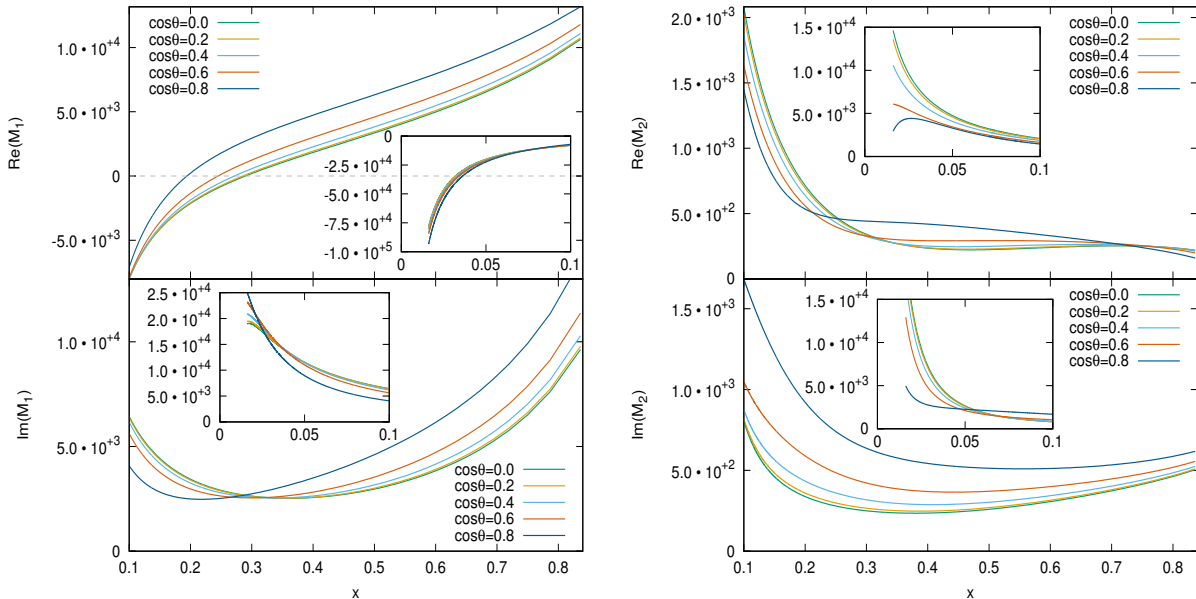


Figure 3: Behavior of $\mathcal{M}_1^{B,(2),fin}$ (left) and $\mathcal{M}_2^{B,(2),fin}$ (right) as a function of the scaling variable x for different values of $\cos(\theta)$. The insets show the region close to $x = 0$.

In Fig. 3, we display the real and imaginary parts of the amplitude $\mathcal{M}_1^{B,(2),fin}$ (left panel) and $\mathcal{M}_2^{B,(2),fin}$ (right panel). The behavior of the amplitudes close to the production threshold, $x = 0$, is shown in the insets. We see that the finite parts of the two-loop amplitude shows stable behavior, and they display a non-trivial dependence on the process kinematics.

In the numerical evaluations, the large rational coefficients of the classical polylogarithms can introduce numerical instabilities in case we do not demand high enough precision. In particular, there are large cancellations between the numerator and denominator of rational functions. Therefore, we evaluate the polylogarithms at double, and the rational coefficients at even higher precision.

5 Discussion and Conclusions

The two-loop massless corrections to the $g + g \rightarrow H + H$ amplitude derived above complete the set of purely virtual amplitudes required for the prediction of the N³LO corrections to Higgs boson pair production in gluon fusion, in the infinite top quark mass limit. All other amplitudes relevant at this order are either (class-A) known already from the calculation of inclusive gluon fusion Higgs boson production at N³LO [68, 69] or (class-B) amount to one-loop and tree-level amplitudes that can be computed using automated tools. The combination of these amplitudes into a fully differential N³LO calculation of Higgs boson pair production does still require substantial advances in the techniques for handling in-

frared singular real radiation configurations at this order, with first steps being taken most recently [70, 71].

More imminent applications of the newly derived results to Higgs boson pair production are the computation of fixed order soft-virtual corrections to the total cross section or of the hard matching coefficients in the resummation of corrections at low pair transverse momentum.

In this paper, we have computed all virtual amplitudes that contribute to the production of a pair of Higgs bosons from the gluon-gluon initiated partonic processes at order a_s^4 . The calculation is performed in an effective field theory where the top quark is integrated out, and all other quarks are massless. The exact calculation of top quark mass effects is currently out of reach at this order, but reweighting procedures allow to reliably quantify these effects [32]. We deal with two classes of amplitudes separately, named class-A (one effective operator insertion) and class-B (two effective operator insertions). The amplitudes of class-A can be related to the gluon form factor which is already known up to three loop order while amplitudes of class-B were known previously up to one loop. Our explicit computation of the two-loop corrections to the class-B amplitudes now completes the perturbative expansion of the $g + g \rightarrow H + H$ amplitude to order a_s^4 . We observe that the pole structure of the amplitude is in agreement with predictions from infrared factorization, and provide (as ancillary files with the arXiv submission of this article) a numerical code to evaluate its finite remainder piece. The newly derived amplitudes open up opportunities for a new level of precision phenomenology predictions in Higgs boson pair production.

Acknowledgements

We would like to thank Claude Duhr, Anirban Karan, Narayan Rana, Lorenzo Tancredi and Andreas von Manteuffel for several useful discussions. This research was supported in part by the Swiss National Science Foundation (SNF) under contract 200020-175595, by the Pauli Center for Theoretical Studies and by the Research Executive Agency (REA) of the European Union under the ERC Advanced Grant MC@NNLO (340983) and ERC Starting Grant MathAm (39568).

References

- [1] ATLAS collaboration, G. Aad et al., *Observation of a new particle in the search for the Standard Model Higgs boson with the ATLAS detector at the LHC*, *Phys. Lett.* **B716** (2012) 1–29, [[1207.7214](#)].
- [2] CMS collaboration, S. Chatrchyan et al., *Observation of a new boson at a mass of 125 GeV with the CMS experiment at the LHC*, *Phys. Lett.* **B716** (2012) 30–61, [[1207.7235](#)].
- [3] C. Englert, A. Freitas, M. M. Mühlleitner, T. Plehn, M. Rauch, M. Spira and K. Walz, *Precision Measurements of Higgs Couplings: Implications for New Physics Scales*, *J. Phys.* **G41** (2014) 113001, [[1403.7191](#)].
- [4] S. Dawson, S. Dittmaier and M. Spira, *Neutral Higgs boson pair production at hadron colliders: QCD corrections*, *Phys. Rev.* **D58** (1998) 115012, [[hep-ph/9805244](#)].

- [5] A. Djouadi, W. Kilian, M. Mühlleitner and P. M. Zerwas, *Testing Higgs selfcouplings at e^+e^- linear colliders*, *Eur. Phys. J. C* **10** (1999) 27–43, [[hep-ph/9903229](#)].
- [6] A. Djouadi, W. Kilian, M. Mühlleitner and P. M. Zerwas, *Production of neutral Higgs boson pairs at LHC*, *Eur. Phys. J. C* **10** (1999) 45–49, [[hep-ph/9904287](#)].
- [7] M. M. Mühlleitner, *Higgs particles in the standard model and supersymmetric theories*, Ph.D. thesis, Hamburg U., 2000. [[hep-ph/0008127](#)].
- [8] E. W. N. Glover and J. J. van der Bij, *Higgs boson pair production via gluon fusion*, *Nucl. Phys. B* **309** (1988) 282–294.
- [9] T. Plehn, M. Spira and P. M. Zerwas, *Pair production of neutral Higgs particles in gluon-gluon collisions*, *Nucl. Phys. B* **479** (1996) 46–64, [[hep-ph/9603205](#)].
- [10] J. Baglio, A. Djouadi, R. Gröber, M. M. Mühlleitner, J. Quevillon and M. Spira, *The measurement of the Higgs self-coupling at the LHC: theoretical status*, *JHEP* **04** (2013) 151, [[1212.5581](#)].
- [11] V. Barger, L. L. Everett, C. B. Jackson and G. Shaughnessy, *Higgs-Pair Production and Measurement of the Triscalar Coupling at LHC(8,14)*, *Phys. Lett. B* **728** (2014) 433–436, [[1311.2931](#)].
- [12] M. J. Dolan, C. Englert and M. Spannowsky, *Higgs self-coupling measurements at the LHC*, *JHEP* **10** (2012) 112, [[1206.5001](#)].
- [13] A. Papaefstathiou, L. L. Yang and J. Zurita, *Higgs boson pair production at the LHC in the $b\bar{b}W^+W^-$ channel*, *Phys. Rev. D* **87** (2013) 011301, [[1209.1489](#)].
- [14] D. E. Ferreira de Lima, A. Papaefstathiou and M. Spannowsky, *Standard model Higgs boson pair production in the $(b\bar{b})(b\bar{b})$ final state*, *JHEP* **08** (2014) 030, [[1404.7139](#)].
- [15] J. K. Behr, D. Bortoletto, J. A. Frost, N. P. Hartland, C. Issever and J. Rojo, *Boosting Higgs pair production in the $b\bar{b}b\bar{b}$ final state with multivariate techniques*, *Eur. Phys. J. C* **76** (2016) 386, [[1512.08928](#)].
- [16] R. Gröber, M. Mühlleitner and M. Spira, *Higgs Pair Production at NLO QCD for CP-violating Higgs Sectors*, *Nucl. Phys. B* **925** (2017) 1–27, [[1705.05314](#)].
- [17] J. Grigo, J. Hoff, K. Melnikov and M. Steinhauser, *On the Higgs boson pair production at the LHC*, *Nucl. Phys. B* **875** (2013) 1–17, [[1305.7340](#)].
- [18] R. Frederix, S. Frixione, V. Hirschi, F. Maltoni, O. Mattelaer, P. Torrielli, E. Vryonidou and M. Zaro, *Higgs pair production at the LHC with NLO and parton-shower effects*, *Phys. Lett. B* **732** (2014) 142–149, [[1401.7340](#)].
- [19] F. Maltoni, E. Vryonidou and M. Zaro, *Top-quark mass effects in double and triple Higgs production in gluon-gluon fusion at NLO*, *JHEP* **11** (2014) 079, [[1408.6542](#)].
- [20] G. Degrossi, P. P. Giardino and R. Gröber, *On the two-loop virtual QCD corrections to Higgs boson pair production in the Standard Model*, *Eur. Phys. J. C* **76** (2016) 411, [[1603.00385](#)].
- [21] R. Gröber, A. Maier and T. Rauh, *Reconstruction of top-quark mass effects in Higgs pair production and other gluon-fusion processes*, *JHEP* **03** (2018) 020, [[1709.07799](#)].
- [22] R. Bonciani, G. Degrossi, P. P. Giardino and R. Gröber, *Analytical Method for Next-to-Leading-Order QCD Corrections to Double-Higgs Production*, *Phys. Rev. Lett.* **121** (2018) 162003, [[1806.11564](#)].

- [23] S. Borowka, N. Greiner, G. Heinrich, S. Jones, M. Kerner, J. Schlenk, U. Schubert and T. Zirke, *Higgs Boson Pair Production in Gluon Fusion at Next-to-Leading Order with Full Top-Quark Mass Dependence*, *Phys. Rev. Lett.* **117** (2016) 012001, [[1604.06447](#)].
- [24] S. Borowka, N. Greiner, G. Heinrich, S. P. Jones, M. Kerner, J. Schlenk and T. Zirke, *Full top quark mass dependence in Higgs boson pair production at NLO*, *JHEP* **10** (2016) 107, [[1608.04798](#)].
- [25] D. de Florian and J. Mazzitelli, *Two-loop virtual corrections to Higgs pair production*, *Phys. Lett.* **B724** (2013) 306–309, [[1305.5206](#)].
- [26] J. Grigo, J. Hoff and M. Steinhauser, *Higgs boson pair production: top quark mass effects at NLO and NNLO*, *Nucl. Phys.* **B900** (2015) 412–430, [[1508.00909](#)].
- [27] D. de Florian and J. Mazzitelli, *Higgs Boson Pair Production at Next-to-Next-to-Leading Order in QCD*, *Phys. Rev. Lett.* **111** (2013) 201801,
- [28] J. Grigo, K. Melnikov and M. Steinhauser, *Virtual corrections to Higgs boson pair production in the large top quark mass limit*, *Nucl. Phys.* **B888** (2014) 17–29, [[1408.2422](#)].
- [29] Q. Li, Q.-S. Yan and X. Zhao, *Higgs Pair Production: Improved Description by Matrix Element Matching*, *Phys. Rev.* **D89** (2014) 033015, [[1312.3830](#)].
- [30] P. Maierhöfer and A. Papaefstathiou, *Higgs Boson pair production merged to one jet*, *JHEP* **03** (2014) 126, [[1401.0007](#)].
- [31] D. de Florian and J. Mazzitelli, *Higgs pair production at next-to-next-to-leading logarithmic accuracy at the LHC*, *JHEP* **09** (2015) 053, [[1505.07122](#)].
- [32] M. Grazzini, G. Heinrich, S. Jones, S. Kallweit, M. Kerner, J. M. Lindert and J. Mazzitelli, *Higgs boson pair production at NNLO with top quark mass effects*, *JHEP* **05** (2018) 059, [[1803.02463](#)].
- [33] D. Y. Shao, C. S. Li, H. T. Li and J. Wang, *Threshold resummation effects in Higgs boson pair production at the LHC*, *JHEP* **07** (2013) 169, [[1301.1245](#)].
- [34] A. Djouadi, M. Spira and P. M. Zerwas, *Production of Higgs bosons in proton colliders: QCD corrections*, *Phys. Lett.* **B264** (1991) 440–446.
- [35] M. Kramer, E. Laenen and M. Spira, *Soft gluon radiation in Higgs boson production at the LHC*, *Nucl. Phys.* **B511** (1998) 523–549, [[hep-ph/9611272](#)].
- [36] K. G. Chetyrkin, B. A. Kniehl and M. Steinhauser, *Hadronic Higgs decay to order α_s^4* , *Phys. Rev. Lett.* **79** (1997) 353–356, [[hep-ph/9705240](#)].
- [37] M. Spira, *Effective Multi-Higgs Couplings to Gluons*, *JHEP* **10** (2016) 026, [[1607.05548](#)].
- [38] M. Gerlach, F. Herren and M. Steinhauser, *Wilson coefficients for Higgs boson production and decoupling relations to $\mathcal{O}(\alpha_s^4)$* , [1809.06787](#).
- [39] P. A. Baikov, K. G. Chetyrkin, A. V. Smirnov, V. A. Smirnov and M. Steinhauser, *Quark and gluon form factors to three loops*, *Phys. Rev. Lett.* **102** (2009) 212002, [[0902.3519](#)].
- [40] T. Gehrmann, E. W. N. Glover, T. Huber, N. Iqizlerli and C. Studerus, *Calculation of the quark and gluon form factors to three loops in QCD*, *JHEP* **06** (2010) 094, [[1004.3653](#)].
- [41] M. F. Zoller, *On the renormalization of operator products: the scalar gluonic case*, *JHEP* **04** (2016) 165, [[1601.08094](#)].

- [42] N. K. Nielsen, *Gauge Invariance and Broken Conformal Symmetry*, *Nucl. Phys.* **B97** (1975) 527–540.
- [43] V. P. Spiridonov and K. G. Chetyrkin, *Nonleading mass corrections and renormalization of the operators $m\psi\psi$ and $G_{\mu\nu}^2$* , *Sov. J. Nucl. Phys.* **47** (1988) 522–527.
- [44] A. L. Kataev, N. V. Krasnikov and A. A. Pivovarov, *Two Loop Calculations for the Propagators of Gluonic Currents*, *Nucl. Phys.* **B198** (1982) 508–518, [[hep-ph/9612326](#)].
- [45] S. Catani, *The Singular behavior of QCD amplitudes at two loop order*, *Phys. Lett.* **B427** (1998) 161–171, [[hep-ph/9802439](#)].
- [46] G. F. Sterman and M. E. Tejeda-Yeomans, *Multiloop amplitudes and resummation*, *Phys. Lett.* **B552** (2003) 48–56, [[hep-ph/0210130](#)].
- [47] T. Becher and M. Neubert, *Infrared singularities of scattering amplitudes in perturbative QCD*, *Phys. Rev. Lett.* **102** (2009) 162001, [[0901.0722](#)].
- [48] E. Gardi and L. Magnea, *Factorization constraints for soft anomalous dimensions in QCD scattering amplitudes*, *JHEP* **03** (2009) 079, [[0901.1091](#)].
- [49] P. Nogueira, *Automatic Feynman graph generation*, *J. Comput. Phys.* **105** (1993) 279–289.
- [50] J. A. M. Vermaseren, *New features of FORM*, [math-ph/0010025](#).
- [51] A. von Manteuffel and C. Studerus, *Reduze 2 - Distributed Feynman Integral Reduction*, [1201.4330](#).
- [52] T. Gehrmann, A. von Manteuffel, L. Tancredi and E. Weihs, *The two-loop master integrals for $q\bar{q} \rightarrow VV$* , *JHEP* **06** (2014) 032, [[1404.4853](#)].
- [53] F. Cascioli, T. Gehrmann, M. Grazzini, S. Kallweit, P. Maierhöfer, A. von Manteuffel, S. Pozzorini, D. Rathlev, L. Tancredi and E. Weihs, *ZZ production at hadron colliders in NNLO QCD*, *Phys. Lett.* **B735** (2014) 311–313, [[1405.2219](#)].
- [54] T. Gehrmann, M. Grazzini, S. Kallweit, P. Maierhöfer, A. von Manteuffel, S. Pozzorini, D. Rathlev and L. Tancredi, *W^+W^- Production at Hadron Colliders in Next to Next to Leading Order QCD*, *Phys. Rev. Lett.* **113** (2014) 212001, [[1408.5243](#)].
- [55] F. Caola, J. M. Henn, K. Melnikov, A. V. Smirnov and V. A. Smirnov, *Two-loop helicity amplitudes for the production of two off-shell electroweak bosons in quark-antiquark collisions*, *JHEP* **11** (2014) 041, [[1408.6409](#)].
- [56] T. Gehrmann, A. von Manteuffel and L. Tancredi, *The two-loop helicity amplitudes for $q\bar{q}' \rightarrow V_1V_2 \rightarrow 4$ leptons*, *JHEP* **09** (2015) 128, [[1503.04812](#)].
- [57] A. von Manteuffel and L. Tancredi, *The two-loop helicity amplitudes for $gg \rightarrow V_1V_2 \rightarrow 4$ leptons*, *JHEP* **06** (2015) 197, [[1503.08835](#)].
- [58] F. Caola, J. M. Henn, K. Melnikov, A. V. Smirnov and V. A. Smirnov, *Two-loop helicity amplitudes for the production of two off-shell electroweak bosons in gluon fusion*, *JHEP* **06** (2015) 129, [[1503.08759](#)].
- [59] F. V. Tkachov, *A Theorem on Analytical Calculability of Four Loop Renormalization Group Functions*, *Phys. Lett.* **100B** (1981) 65–68.
- [60] K. G. Chetyrkin and F. V. Tkachov, *Integration by Parts: The Algorithm to Calculate beta Functions in 4 Loops*, *Nucl. Phys.* **B192** (1981) 159–204.

- [61] T. Gehrmann and E. Remiddi, *Differential equations for two loop four point functions*, *Nucl. Phys.* **B580** (2000) 485–518, [[hep-ph/9912329](#)].
- [62] S. Laporta, *High precision calculation of multiloop Feynman integrals by difference equations*, *Int. J. Mod. Phys.* **A15** (2000) 5087–5159, [[hep-ph/0102033](#)].
- [63] C. Anastasiou and A. Lazopoulos, *Automatic integral reduction for higher order perturbative calculations*, *JHEP* **07** (2004) 046, [[hep-ph/0404258](#)].
- [64] A. V. Smirnov, *Algorithm FIRE – Feynman Integral REduction*, *JHEP* **10** (2008) 107, [[0807.3243](#)].
- [65] C. Studerus, *Reduze-Feynman Integral Reduction in C++*, *Comput. Phys. Commun.* **181** (2010) 1293–1300, [[0912.2546](#)].
- [66] R. N. Lee, *LiteRed 1.4: a powerful tool for reduction of multiloop integrals*, *J. Phys. Conf. Ser.* **523** (2014) 012059, [[1310.1145](#)].
- [67] T. Gehrmann, L. Tancredi and E. Weihs, *Two-loop master integrals for $q\bar{q} \rightarrow VV$: the planar topologies*, *JHEP* **08** (2013) 070, [[1306.6344](#)].
- [68] C. Anastasiou, C. Duhr, F. Dulat, F. Herzog and B. Mistlberger, *Higgs Boson Gluon-Fusion Production in QCD at Three Loops*, *Phys. Rev. Lett.* **114** (2015) 212001, [[1503.06056](#)].
- [69] B. Mistlberger, *Higgs boson production at hadron colliders at N^3LO in QCD*, *JHEP* **05** (2018) 028, [[1802.00833](#)].
- [70] J. Currie, T. Gehrmann, E. W. N. Glover, A. Huss, J. Niehues and A. Vogt, *N^3LO corrections to jet production in deep inelastic scattering using the Projection-to-Born method*, *JHEP* **05** (2018) 209, [[1803.09973](#)].
- [71] L. Cieri, X. Chen, T. Gehrmann, E. W. N. Glover and A. Huss, *Higgs boson production at the LHC using the q_T subtraction formalism at N^3LO QCD*, [[1807.11501](#)].